NEOPLASIA
www.neoplasia.com

Volume 20 Number 10 October 2018 pp. 975–984 975

A Novel Method for Quantifying Total Thoracic Tumor Burden in Mice[1]

Pavitra Viswanath[*†], Shaohua Peng[*], Ratnakar Singh[*2], Charles Kingsley[‡], Peter A. Balter[§] and Faye M. Johnson[*†]

[*]Department of Thoracic Head & Neck Medical Oncology, The University of Texas MD Anderson Cancer Center, Houston, TX; [†]The University of Texas Graduate School of Biomedical Sciences, Houston, TX; [‡]Department of Imaging Physics, The University of Texas MD Anderson Cancer Center, Houston, TX; [§]Department of Radiation Physics, The University of Texas MD Anderson Cancer Center, Houston, TX

Abstract

Mouse models are powerful tools to study lung cancer initiation and progression *in vivo* and have contributed significantly to recent advances in therapy. Using micro-computed tomography to monitor and study parenchymal and extra-parenchymal metastases in existing murine models of lung cancer is challenging owing to a lack of radiographic contrast and difficulty in achieving respiratory gating. To facilitate the analysis of these *in vivo* imaging studies and study of tumor progression in murine models we developed a novel, rapid, semi-automated method of calculating thoracic tumor burden from computed tomography images. This method, in which commercially available software is used to calculate the mass of the thoracic cavity (MTC), takes into account the aggregate tumor burden in the thoracic cavity. The present study showed that in tumor-free mice, the MTC does not change over time and is not affected by breathing, whereas in tumor-bearing mice, the increase in the MTC is a measure of tumor mass that correlates well with tumor burden measured by lung weight. Tumor burden calculated with our MTC method correlated with that measured by lung weight as well as or better than that calculated using four established methods. To test this method, we assessed metastatic tumor development and response to a pharmacologic PLK1 inhibitor in an orthotopic xenograft mouse model. PLK1 inhibition significantly inhibited tumor growth. Our results demonstrate that the MTC method can be used to study dynamic changes in tumor growth and response to therapeutics in genetically engineered mouse models and orthotopic xenograft mouse models of lung cancer.

Neoplasia (2018) 20, 975–984

Abbreviations: DICOM, Digital Imaging and Communications in Medicine; GEMM, genetically engineered mouse model; KP, KRAS TP53; micro-CT, micro–computed tomography; MTC, mass of the thoracic cavity; PLK1, polo-like kinase 1; RECIST, Response Evaluation Criteria in Solid Tumors; ROI, region of interest; SCP, sum of cross-product; T&V, tumor and vessel volume.

Address all correspondence to: Faye M. Johnson, Department of Thoracic Head & Neck Medical Oncology, Unit 432, The University of Texas MD Anderson Cancer Center, 1515 Holcombe Blvd, Houston, TX 77030, USA.
E-mail:; fmjohns@mdanderson.org

[1] Funding: MD Anderson's animal facilities are supported by the National Institutes of Health through MD Anderson's Cancer Center Support Grant (P30CA016672). This work was supported by individual donations (FMJ) and by the Office of the Assistant Secretary of Defense for Health Affairs through the Lung Cancer Research Program (award no. W81XWH-17-1-0206). Opinions, interpretations, conclusions, and recommendations are those of the authors and are not necessarily endorsed by the Department of Defense.

[2] Present address: Department of Comparative Biosciences, University of Illinois Urbana-Champaign, Champaign, Illinois.

Received 26 June 2018; Accepted 2 August 2018

1476-5586
https://doi.org/10.1016/j.neo.2018.08.003

Introduction

Lung cancer is the second most common cancer in men and women, with about 234,030 American adults being diagnosed with the disease in 2018 alone. Despite advances in its treatment, lung cancer remains the leading cause of cancer death [1]; patients have a five-year survival rate of less than 15%. The development of better lung cancer therapies requires a deeper understanding of the molecular signaling mechanisms that drive the disease's formation, maintenance, and progression. Cancer disease progression studies are very important in assessing response-guided treatment strategies in patients with solid tumors as they allow for clinical trial analysis to calculate time-to-event endpoints and more importantly, assist in determining clinical treatment response and/or failure.

In vivo studies in murine models play important roles in identifying the mechanisms of lung tumorigenesis and assessing the safety and efficacy of novel drug therapies. The models most commonly used to study lung tumorigenesis and therapeutic strategies are subcutaneous xenograft models created by implanting human cell lines or patient tissues into immunocompromised mice [2]. However, murine orthotopic models of lung cancer, although technically more challenging than subcutaneous models, have a tumor microenvironment more representative of that in humans, making them better suited for the study of disease progression *in vivo* [3]. Orthotopic models of lung cancer can be generated in immunocompromised or immunocompetent mice by intrabronchial injections [4], intrathoracic injections [5], tail vein injections that result in lung metastasis [6], or percutaneous injections of lung cancer cells into the left lung [7]. Most genetically engineered mouse models (GEMMs) have the advantages of being orthotopic and having an intact immune system. Many GEMMs encompass several mutations found in non–small cell lung cancer (NSCLC), including KRAS, BRAF, EGFR, LKB1, TP53, and NFκB [8]. Most GEMMs of NSCLC are adenocarcinoma models and one of the most commonly used models was established by engineering a Lox-Stop-Lox conditional KRAS G12D mutation in the endogenous KRAS locus [9,10]. Combining KRAS activation with the concomitant inactivation of p53 results in more aggressive tumors that also metastasize. The relationship between primary tumor nodules and individual metastases could be established in studies in which KRAS activation and p53 inactivation are achieved by infecting the mouse lung with lentiviral Cre [11].

The evaluation of lung cancer progression in the lungs of mice is primarily based on end-stage procedures performed after necropsy, such as histopathologically analyzing lung tissue, weighing the lungs, or counting lung tumors. Although these *ex vivo* procedures offer many opportunities to perform molecular and cellular analyses, they are limited to only one measurement and do not provide details about the dynamic processes that occur over time *in vivo*. In contrast, micro–computed tomography (micro-CT) can be used to noninvasively study the dynamic changes of tumor progression in preclinical models [12]. Although micro-CT is technically challenging because of respiratory movement artifacts, it provides visual and quantitative information about the whole lung in a three-dimensional manner with high resolution and sensitivity. More importantly, micro-CT allows for the longitudinal assessment of therapeutic interventions in different treatment groups as well as that of the extent of disease in individual mice. In addition, despite delivering a relatively large radiation dose per acquisition, micro-CT is safe, causing no radiotoxicity to the lungs of mice undergoing weekly micro-CT for up to 12 weeks [13]. However, unlike CT in humans, micro-CT in mice does not include the use of radiographic contrast, and achieving respiratory gating with micro-CT in mice is difficult.

Micro-CT has been successfully used to detect lung tumors and evaluate lung tumor burden in many NSCLC mouse models [14–16]. Methods previously used to quantify metastatic tumor burden relied on Response Evaluation Criteria in Solid Tumors (RECIST)-like assessment, in which the maximal tumor diameter and largest perpendicular diameter were measured in the coronal plane and the tumor burden was calculated from the sum of the cross products [17]. However, such methods may have reader bias, and variability has been observed among readers. In addition, these methods measure only the largest tumors and ignore small tumors that, in aggregate, may contribute significantly to the total tumor burden. Other methods that have been used to quantify tumor burden include tumor nodule segmentation [18]; segmentation of the aerated lung volume with respiratory gating [19]; manual segmentation of the chest space [16]; tracking of individual nodules [20]; modeling of tumors as ellipsoids [21]; and volumetric measurement of the combined tumor and vasculature from a threshold-based region growing algorithm with manual and semi-automated segmentation [22]. However, these methods are labor-intensive, require specific skill sets in radiology, and do not take all thoracic metastases into consideration. Murine micro-CT imaging has limitations that are not present for human CT imaging. As the murine micro-CT imaging is not respiratory gated, the probability of air escaping into the lungs and variance in the breathing period is high despite breath hold at the time of imaging. Also, tumor tissue and vasculature cannot be distinguished in the non-contrast micro-CT imaging as they have similar X-ray densities.

Therefore, we developed a semi-automated, unbiased method of analyzing micro-CT without respiratory gating for the *in vivo* quantitative assessment of lung tumor mass in mice. We propose this imaging technique and tumor mass analysis as a quantitative tool that is reliable and yields dynamic information on disease progression. Given the basic assumption that the aerated mass of the thoracic cavity (MTC) in an adult mouse does not change over time unless disease progresses, our imaging and analysis protocol is designed to permit comparisons between different groups, enable the evaluation of individual animals over time, and provide specific information about disease progression and metastasis. Unlike aerated lung volume, which is dependent upon the respiratory phase of breath hold, MTC is dependent on the differences in density between tumors and parenchymal tissue independent of respiratory state. In the present study, we evaluated our model by comparing its performance with that of with four established methods and a reference method in assessing tumor burden in a murine orthotopic model of metastatic lung cancer.

Materials and Methods

Cells

Highly metastatic 344SQ (miR200-expressing) cells were derived from transgenic mice with KRAS (G12D) TP53 (R172H) mutations (KP mice) [23] and were a generous gift from Dr. Don Gibbons. The cells were maintained in RPMI 1640 with 10% fetal bovine serum in a humidified 5% CO_2 atmosphere at 37°C as described previously [24].

Mice

All animal experiments were conducted in accordance with the laws of the United States and the regulations of the U.S. Department of Agriculture. All animal experiments were reviewed and approved

by the Institutional Animal Care and Use Committee at The University of Texas MD Anderson Cancer Center and conducted in accordance with MD Anderson's Office of Research Administration and Institutional Animal Care and Use Committee guidelines. Four- to six-week-old 129/sv male mice were purchased from Charles River Laboratory (Wilmington, MA). The mice were 8 weeks old at the start of the study. At the end of the study, lungs were embedded in paraffin and stained with hematoxylin and eosin (H&E) to check for the presence of tumor cells as described previously [25].

Murine Orthotopic Model of Lung Cancer

For the creation of the orthotopic model, the mice were first fully anesthetized with 2–4% isoflurane and placed in a right lateral decubitus position. The lower edge of the right rib cage was identified by palpation, and fur in the area was trimmed with a hair clipper. After it was cleaned with 70% ethanol solution, the area was shaved with a razor blade to remove any remaining fur. The incision site was sterilized with povidone-iodine solution. A 1-cm incision was made through the skin along the lower edge of the rib cage. The cephalic edge of the skin was retracted with forceps to reveal the underlying subcutaneous tissue and fat. A second incision was made through the fatty tissue to reveal the rib cage and the thoracic cavity. The respiring lung was identified as a pale structure under the rib cage, whereas the more caudal spleen was identified as a dark red organ. Tumor cells ($2x10^5$ 344SQ cells in 50 µl of serum free medium) were injected into the lower third of the left lung using an insulin syringe. The left lung was then checked to ensure the absence of intra-thoracic hemorrhage or collapse. For the incision closure, the opposing skin was held together with forceps and then closed with two or three 9-mm staples applied with an Autoclip stapler. The mice were then given 0.05–0.10 mg/kg buprenorphine, placed under a heat lamp, and monitored for recovery. Mice were returned to their cages once they were able to move on all four limbs.

Endotracheal Intubation and Micro-CT

Micro-CT imaging of the lungs was carried out to serve as baseline study. For micro-CT, the mice were first placed in an inhalation anesthesia induction chamber and exposed to 5% isoflurane. When the mice were fully anesthetized, a BioLite mouse intubation system (Braintree Scientific) was used to place a 22-gauge, 2.5-cm endotracheal tube. Anesthesia was then maintained with 1.5–3.0% isoflurane. The mice were then placed onto a holder and moved to the micro-CT system (XRAD 225Cx, Precision X-Ray Incorporated, North Branford, CT).The micro-CT parameters used were 60 Kv, 4 mA, and 3 RPM. The mice were mechanically ventilated at 60 BPM throughout the procedure. A 20-second breath hold at 20 cmH_2O was applied during the acquisition as described previously [26]. The pressure was monitored with an inline manometer. After the acquisition was complete, the mice were extubated and allowed to recover in a clean, warm cage.

Murine Drug Therapy

In order to validate the ability to noninvasively record patterns of lung tumor growth and response to therapy in orthotopically injected tumors, mice bearing 344SQ tumors were treated with intraperitoneal injections of vehicle only or 30 mg/kg volasertib (Selleck Chemicals, Houston, TX) once per week for 3 weeks to evaluate anticancer efficacy. Micro-CT was performed before injection (baseline) and then once per week for 3 weeks until the end of the study.

CT Image Analysis: MTC Method

The micro-CT images were exported in Digital Imaging and Communications in Medicine (DICOM) format. The DICOM image sequence was uploaded to the RayStation 5.0.2 treatment planning system (Raysearch, Sweden). The lung volume was determined based on a growing algorithm using a threshold of −800 to 0 HU to remove bias. A region of interest (ROI) in the chest cavity was drawn from the base of the lungs to the top of the trachea using RayStation's smart contour option. The MTC was calculated as a function of ROI volume and CT intensity. Tumor mass was determined by comparing the MTC of the diseased mice with the aerated MTC calculated from the baseline micro-CT images.

CT Image Analysis: Sum of Cross-Product Method

The quantification of tumor burden by the manual sum of cross-product (SCP) analysis of the micro-CT images was performed as described previously [17]. The SCP method is very similar to RECIST, a standardized measure of tumor response, especially in clinical trials [27]. The lung micro-CT DICOM images were viewed using the Fiji distribution of the NIH ImageJ software program (http://fiji.sc/Fiji). The tumors were visualized in the coronal plane, and the largest cross-sectional plane of each tumor was identified. A ruler was placed on the screen to measure the maximal tumor diameter (d_1) and largest perpendicular tumor diameter (d_2). The total tumor burden was then determined by calculating the SCP ($SCP = \sum[d_1 * d_2]$) of all tumors per animal. This method has been validated by *ex vivo* micro-CT analysis [17,28].

CT Image Analysis: Tumor and Vessel Volume Method

Tumor and vessel volume (T&V) was calculated as described previously [22]. In brief, the functional lung volume was calculated based on a region growing algorithm with the threshold value set at [−800 to 0 HU], these values were chosen empirically based on the visual inspection of a few mice on the RayStation system. The total chest space volume excluding the heart was calculated using the region growing algorithm and semi-automated contouring. The combined T&V was determined by subtracting the functional lung volume from the total chest space volume [22].

CT Image Analysis: Ellipsoidal Tumor Volume Method

The micro-CT images were viewed using the MicroView 2.2 software program (GE Healthcare). One to five tumors in each mouse were identified and selected on the axial view. The three greatest diameters of each tumor on the axial, coronal, and sagittal views (referred to as x, y, and z, respectively) were measured. These values were then used to calculate the volume of the tumor using the formula for determining the volume of an ellipsoid ($[4\pi/3][x/2][y/2][z/2]$) [29–31].

CT Image Analysis: Aerated Lung Volume Method

Functional lung volume measurement, a fully automated method that utilizes gray-level, morphological, and texture features to segment the aerated lung region using a region growing algorithm, was performed as described previously [19]. Measurement of the functional lung volume is an inverse surrogate measure of tumor burden [19]. Owing to the lack of respiratory gating facility, the aerated lung volume was measured immediately before mice were euthanized on day 33.

Statistical Analysis

Statistical analysis was carried out using GraphPad Prism 7 software (GraphPad, La Jolla, CA). One-way analysis of variance and the Tukey's multiple comparison test were used to assess changes in the MTCs of the disease-free mice over time in comparison to baseline. Pearson correlation was used to compare tumor burden calculated using the different

methods with lung weight and with MTC method. All data values presented are mean ± standard deviation (SD), and the error bars on the graphs represent standard error of mean (SEM).

Results

The MTCs of Adult Mice Do Not Change Over Time

To test the assumption that the aerated MTC does not change over time unless the tumor burden changes, we periodically imaged five non–tumor-bearing mice using the same schedule as that used for the tumor-bearing mice and calculated the MTC. The MTCs of non–tumor-bearing mice did not change over time (Figure 1, *A* and *B*); the percent change in MTC was 0 ± 0.2 ($P > .99$). No changes in MTC were observed despite the mice being at different breath hold stages during image acquisition.

However, aerated lung volume in the same mice varied significantly over time, likely because the breath holds for the imaging were initiated at random respiratory states (Figure 1*C*). The

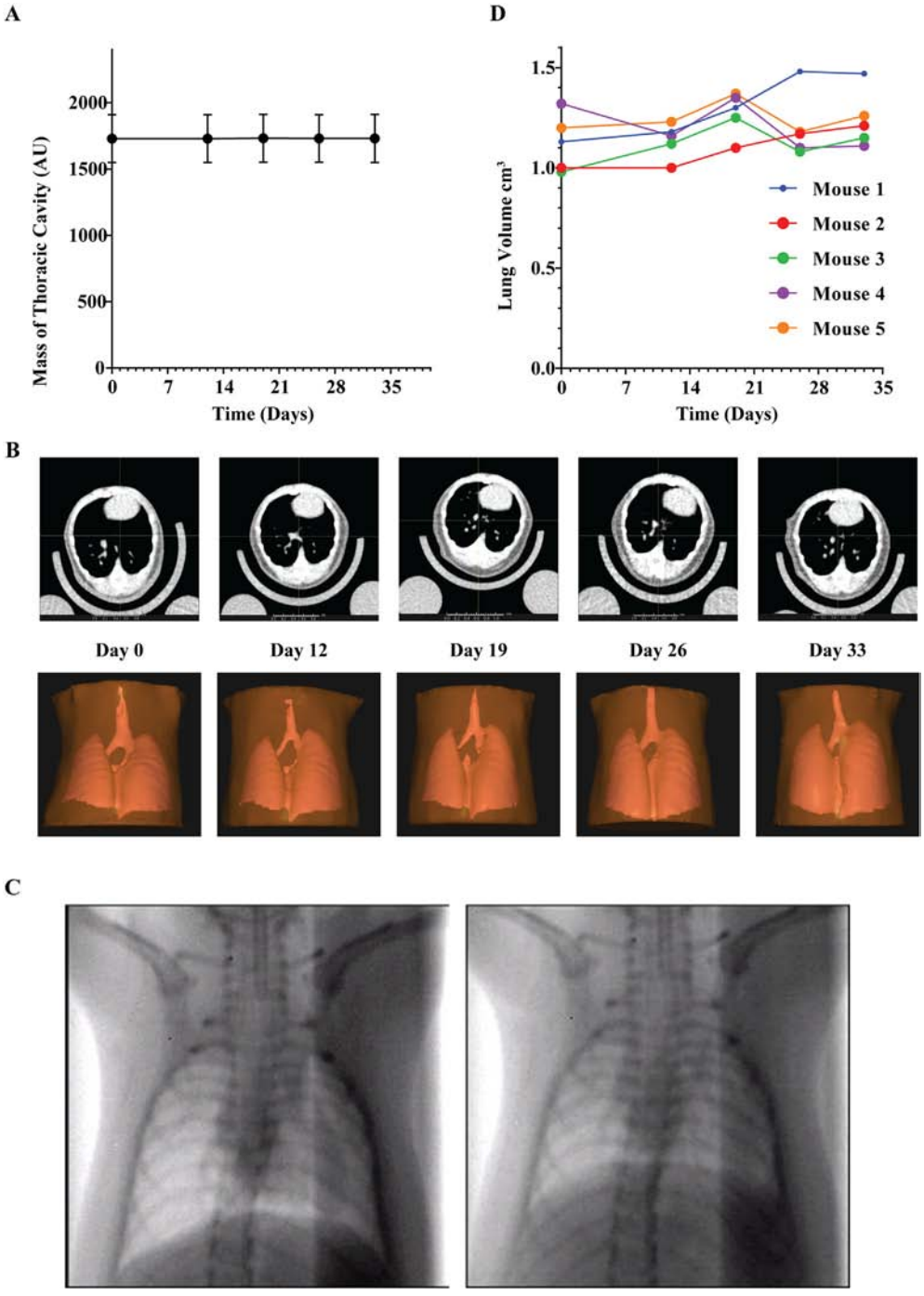

Figure 1. The MTC does not change over time in tumor-free mice. **(A)** The MTCs of five non–tumor-bearing mice were calculated over time as a product of volume and intensity. The error bars show standard deviations. **(B)** Representative micro-CT images (upper panel) and MTCs (lower panel) of non–tumor-bearing mice over time. **(C)** Representative scout images of breath hold in mice after tracheal intubation. **(D)** Aerated lung volumes of non–tumor-bearing mice over time. AU, arbitrary units.

percent changes in lung volume on days 12, 19, 26, and 33 were 1.8 ± 9.5, 13.8 ± 9.2, 8.0 ± 18.1, and 11.5 ± 17.8, respectively (Figure 1*D*). This substantial variability suggests that the measured aerated lung volume does not accurately depict disease progression over time.

Quantitative Measurement of Lung Tumor Mass in a Murine Orthotopic Lung Cancer Model Accurately Determines Tumor Burden

Eleven mice were imaged at baseline and the MTC was calculated. 344SQ murine lung adenocarcinoma cells were then injected into the left lung of the mice *via* orthotopic injection. The mice were then serially imaged on days 12, 19, 26 and 33 to study the course of tumor development and MTC was calculated. The tumor mass was then calculated by subtracting the MTC on the specific day from the baseline MTC (Figure 2*A*). Tumor-bearing mice survived an average of 3 weeks after the 344SQ cell injection. The mice were euthanized when they were moribound or on day 33 immediately after the last micro-CT imaging session. The mice were necropsied, the number of primary and metastatic tumors were counted and the lungs were collected and weighed. The calculated tumor mass was then compared to the gold standard of tumor burden, lung weight. Tumor mass calculated using the MTC method was correlated with lung weight (r = 0.78, P = .005) (Figure 2*B*).

Lung Tumor Burden Measured Using Established Methods Correlates with Lung Weight

We evaluated four other methods of lung tumor burden measurement: the RECIST-like method (SCP) [17]; aerated lung volume [19] without respiratory gating; volumetric measurement of combined tumor and vasculature from a threshold-based region growing algorithm with manual and semi-automated segmentation (T&V) [22]; and the ellipsoid tumor burden measurement [21]. To determine the intrinsic accuracy of each method in determining tumor burden, the tumor burden of the same 10 mice with lung adenocarcinoma was calculated using each method and compared to lung weight. Lung weight correlated with tumor burden measured using the SCP method (r = 0.63, P = .03) (Figure 3*A*), ellipsoid tumor volume method (r = 0.78, P = .004) (Figure 3*B*), T&V method (r = 0.65, P = .02) (Figure 3*C*), and aerated lung volume method (r = −0.69, P = .01) (Figure 3*D*), confirming that these methods can accurately determine tumor burden in mice with lung adenocarcinoma.

Comparison of Methods of Lung Tumor Burden Quantification with MTC Method

The tumor burdens calculated with four established methods were plotted against the tumor mass calculated with our MTC method. Tumor burden calculated using the MTC method correlated significantly with all the methods of tumor burden quantification including the SCP method (r = 0.69, P = .0006) (Figure 4*A*); the ellipsoid tumor volume method (r = 0.62, P = .003) (Figure 4*B*); the T&V method (r = 0.51, P = .01) (Figure 4*C*); and the aerated lung volume method (r = −0.60, P = .0044) (Figure 4*D*). Features of the MTC method, the other four micro-CT analysis methods of tumor burden measurement, and the reference method (lung weight assessment) are shown in Table 1.

Application Study for MTC Method Demonstrates that Volasertib Treatment Reduces Tumor Mass in an Orthotopic Mouse Model of Mesenchymal Metastasis

To test the MTC method in an independent dataset, we assessed the anti-cancer effect of the polo-like kinase 1 (PLK1)

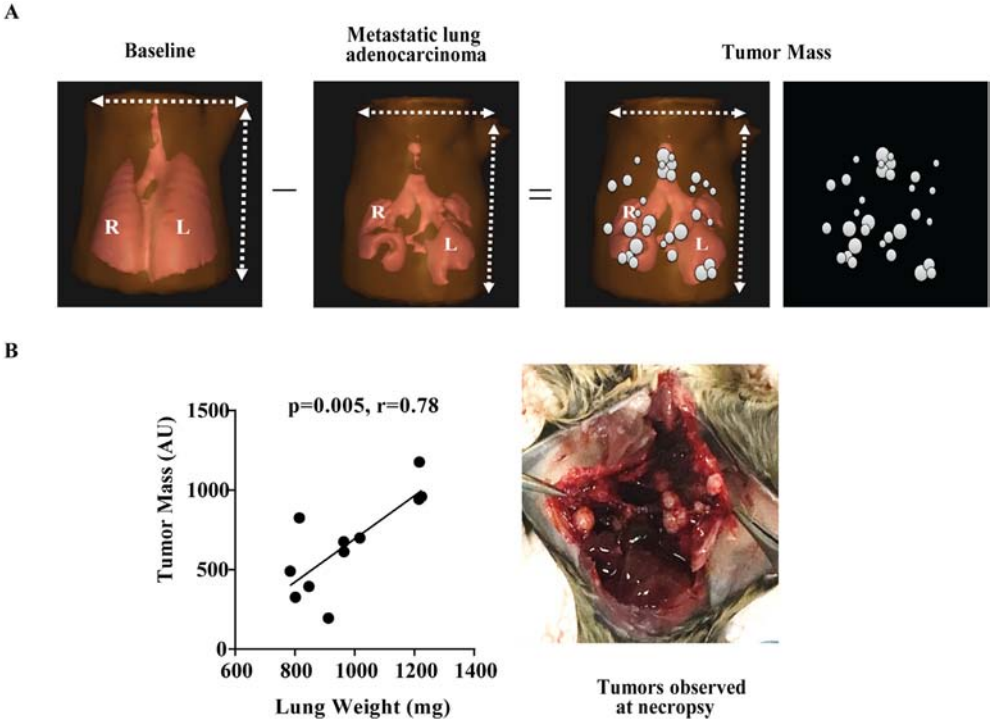

Figure 2. Tumor mass calculated using the MTC method accurately measures thoracic tumor burden in a murine orthotopic model of lung cancer. (**A**) Representative images illustrating the MTC method of calculating tumor burden. The baseline MTC is calculated before cancer cell injection. Tumor mass is calculated by subtracting the MTC of the tumor-bearing mouse from the mouse's baseline MTC. (**B**) Tumor mass calculated using the MTC method on day 33 was correlated with lung weight at the end of the experiment (day 33).

inhibitor volasertib in an orthotopic mouse model. Our previous work suggested that PLK1 inhibition would be effective against mesenchymal NSCLC [32,33]. Epithelial-mesenchymal transition (EMT) is an important process during the progression of lung cancer. Epithelial cells lose the polarity, which contributes to uncontrolled invasion and metastasis of cancer cells. Most lung cancer patients have an extensive array of secondary tumor sites, which are established through the metastatic cascade of which EMT is a direct regulator.

Twenty-five mice were imaged at baseline. We injected 344SQ cells into the left lungs of 20 mice. On day 12 (*i.e.*, 12 days after tumor cell injection), the mice had measurable tumors and were randomized to receive weekly intravenous injections of vehicle only (control) or 30 mg/kg volasertib for 4 weeks. Five mice that did not receive cancer cell injections served as negative controls. All mice were serially imaged on days 12, 19, 26, and 33.

We found significant differences in the tumor mass calculated using the MTC method between the vehicle and volasertib-treated

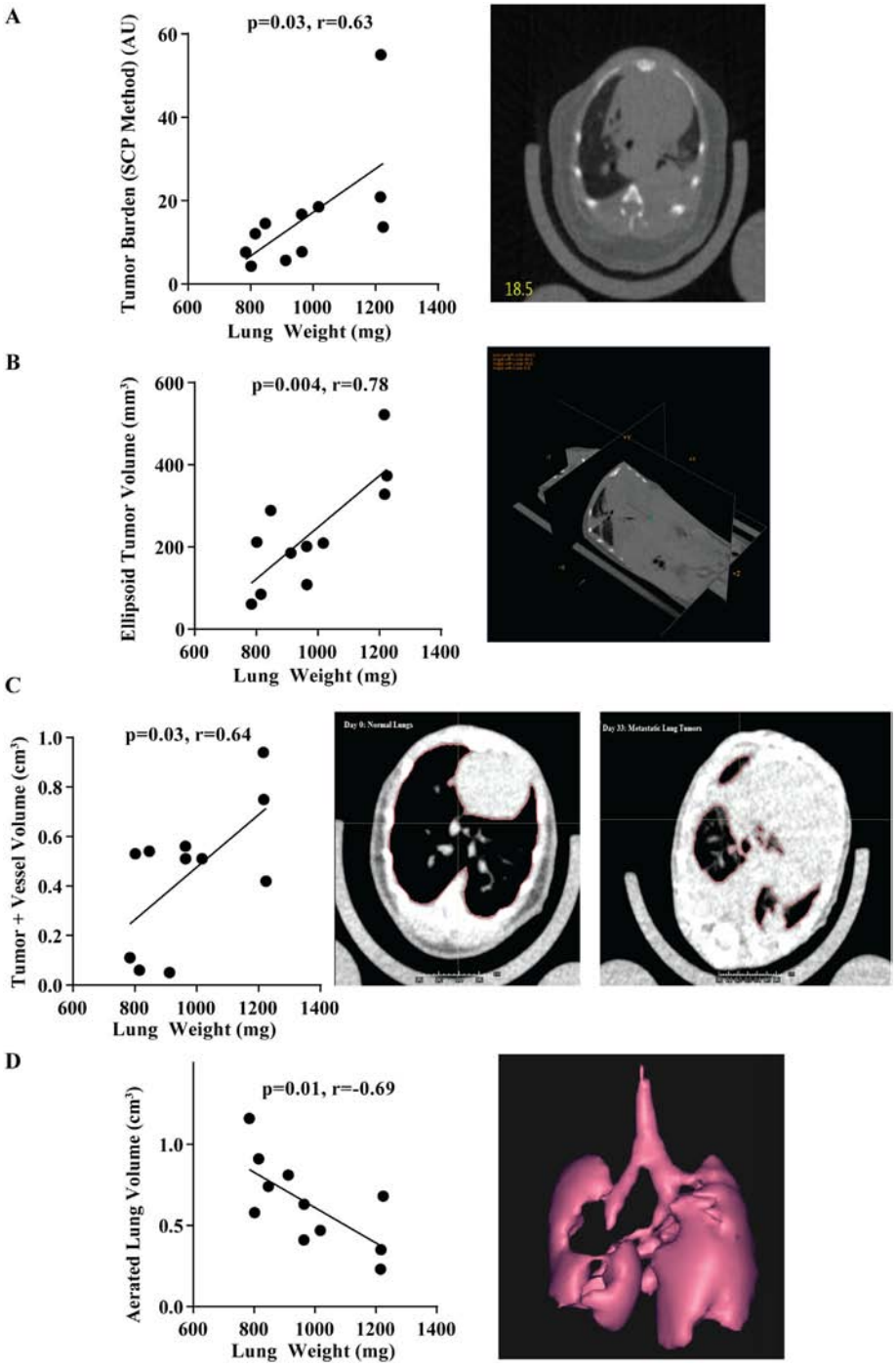

Figure 3. Lung tumor burden assessed using four established methods correlated well with tumor mass estimated using lung weight. Lung weight in 11 mice at the end of the experiment was compared with tumor burden as measured using the SCP (**A),** ellipsoid tumor volume (**B**), T&V (**C**), and aerated lung volume (**D**) methods. Pearson correlation was used to compute the R values. The representative images for calculation of tumor burden for each method is also represented.

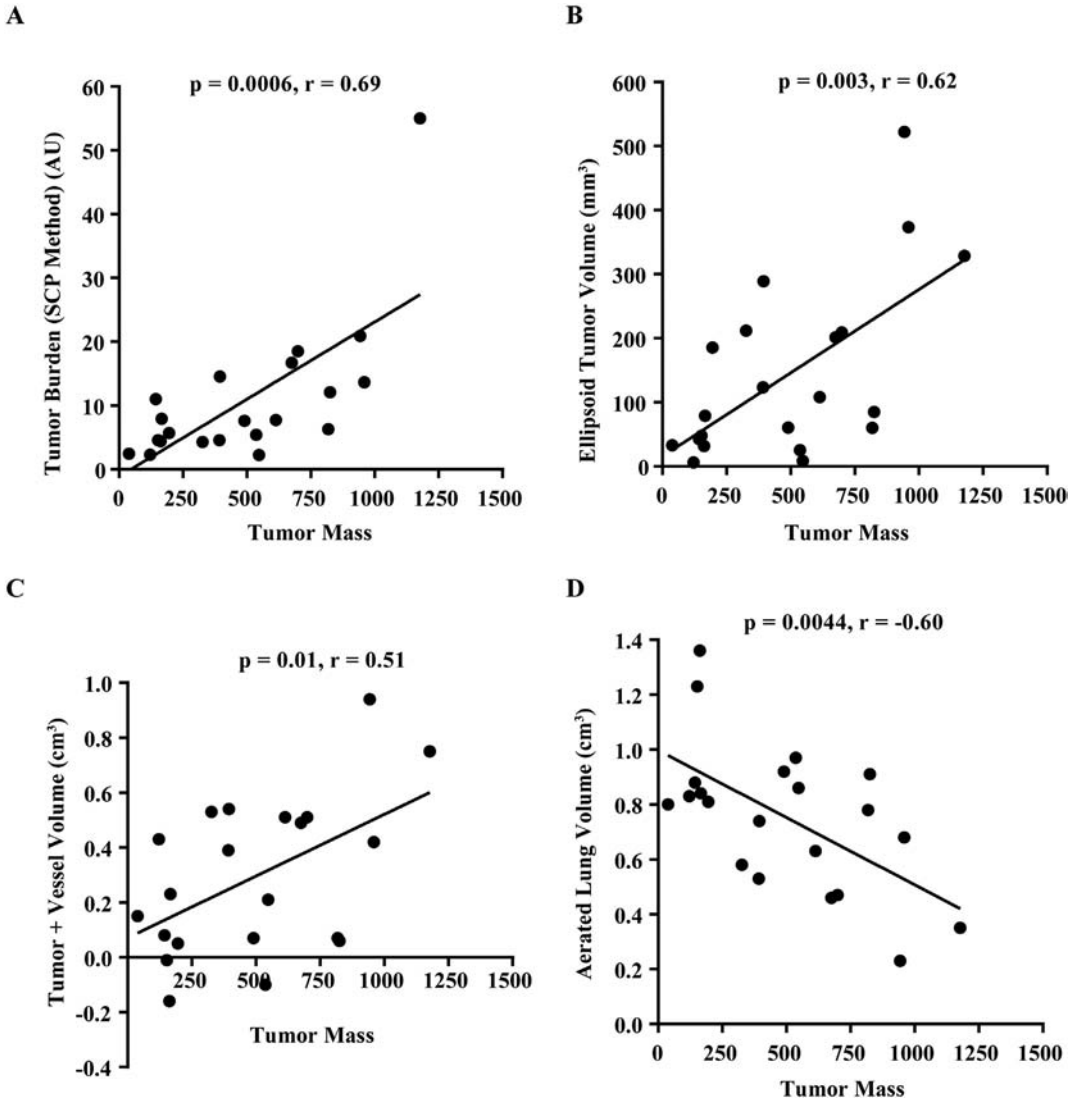

Figure 4. Tumor mass calculated using the MTC method correlated with tumor burden measured using four established techniques. Tumor mass calculated using the MTC method was compared with tumor burden measured using the SCP method (**A**), ellipsoid tumor volume method (**B**), T&V method (**C**), and end point lung volume method (**D**). Pearson correlation was used to compute the R values.

mice on days 19 ($P = .035$), 26 ($P = .008$), and 33 ($P = .004$) (Figure 5*A*). We also found a significant difference in the percent change in tumor mass at day 33 between the control and volasertib-treated mice ($P = .0064$) based on non-parametric Mann–Whitney t-test analysis (Figure 5*B*) depicting tumor regression in the mice treated with volasertib compared to the vehicle control treated mice at the end of the study. All 10 mice treated with volasertib had stable disease or regression, whereas all but one of the 11 control mice had an increase in tumor mass (Figure 5*C*). Hematoxylin and eosin staining of lung tissues collected at the end of treatment showed that the lungs of the control mice had many tumor cells present, whereas the lungs of the volasertib-treated mice had very few tumor cells remaining (Figure 5*D*). Representative images of the control and volasertib-treated mice over time are shown in Figure 5*E*.

Table 1. Comparison of Different Methods of Measuring Lung Tumor Burden

	MTC Method (Study Method)	SCP (RECIST-Like) Method	Ellipsoidal Method	T&V Volume Method	Aerated Lung Volume Method	Lung Weight (Reference Method)
Primary tumor measurement	YES	YES	YES	YES	YES	YES
Metastatic of parenchymal lung tumors	ALL	Largest 5	Largest 5	ALL	ALL	ALL
Measurement of extra-parenchymal thoracic tumors	YES	NO	NO	NO	NO	NO
Dynamic changes in tumor volume or mass	YES	YES	YES	YES	NO	NO
Semi-automated analysis	YES	NO	NO	YES	YES	NO
Dimensional measurement	3D	2D	3D	3D	3D	
Time taken for analysis per mouse	5–8 min	12–15 min	15–20 min	10–15 min	3–5 min	2–5 min
Software/tool used	RayStation	ImageJ	MicroView	RayStation	RayStation	Surgical tools and weighing scale
Correlation with reference method (R value/p value)	0.78/0.005	0.63/0.03	0.78/0.004	0.65/0.02	−0.69/0.01	

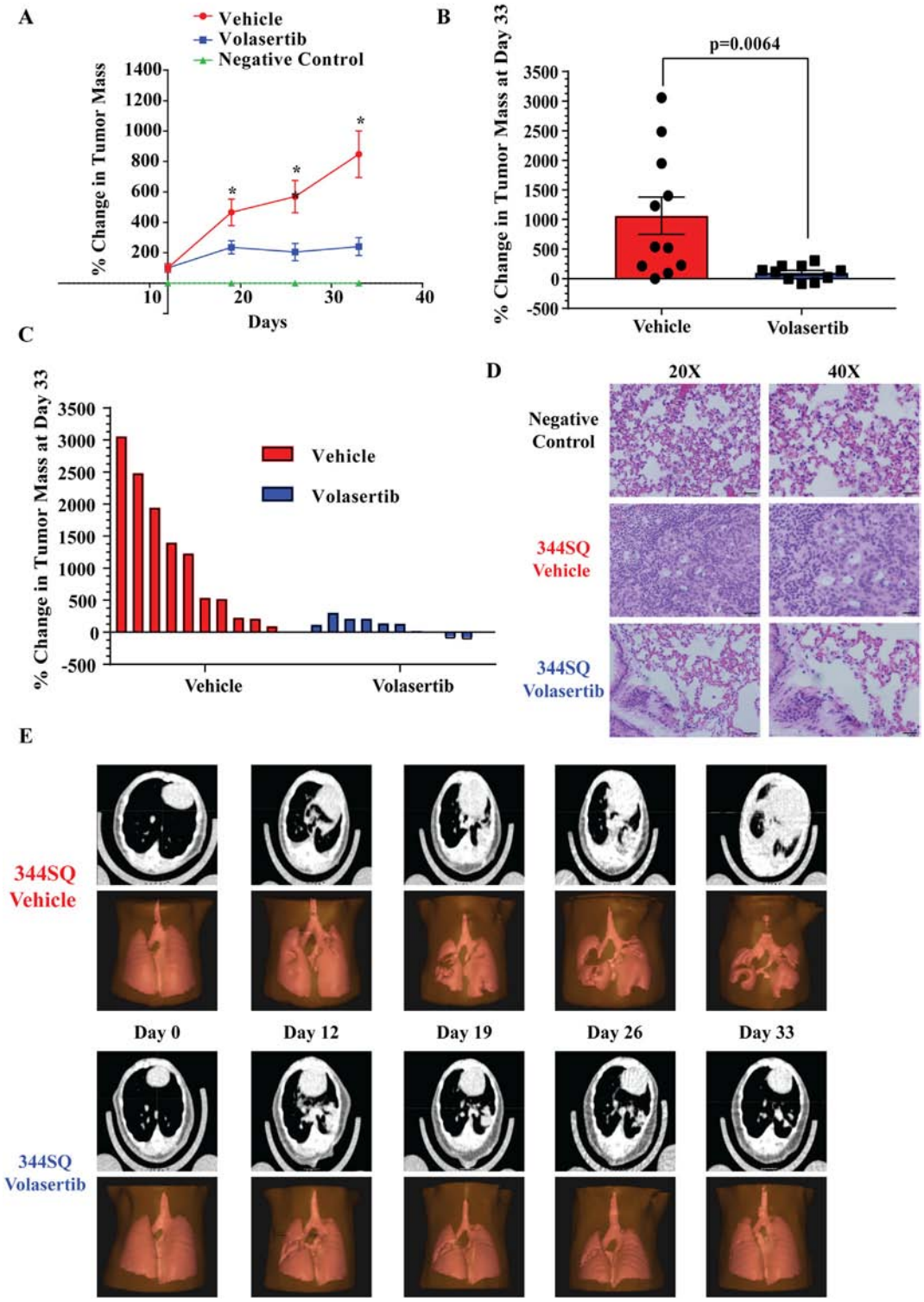

Figure 5. Tumor mass measured with the MTC method accurately reflected the effect of PLK1 inhibition in a murine orthotopic model of mesenchymal metastatic NSCLC. Mice without cancer (negative control) and 344SQ tumor-bearing mice treated with volasertib or vehicle starting on day 12 underwent micro-CT imaging on days 12, 19, 26, and 33 and tumor mass was calculated using the MTC method. **(A–C)** The percent change in tumor mass from day 12 to the indicated time point for each treatment group (**A-B**) and for each individual tumor (**C**). Error bars represent standard deviations. *$P < .05$. Representative hematoxylin and eosin–stained lung sections at the end of the experiment (**D**) and representative micro-CT and 3D MTC images over time (**E**) of negative control mice and mice bearing 344SQ tumors treated with vehicle only or with volasertib are shown.

Discussion

In the current study, we utilized micro-CT imaging in a KRAS/p53-driven orthotopic lung cancer model to monitor lung cancer initiation and progression. We developed a micro-CT image analysis method to quantitatively measure tumor mass as a measure of total thoracic tumor burden in murine lung cancer models. This method of tumor

mass calculation takes into account both the primary and the metastatic tumors present in the thoracic cavity from the base of the lung to the top of the trachea. In addition, we successfully demonstrated the efficacy of PLK1 inhibition in a mesenchymal metastatic lung orthotopic mouse model by using micro-CT imaging. These results highlight the advantage of micro-CT guided analysis that makes it possible to measure tumor development, select animals with a certain range of tumor size, and follow response to drug treatment.

We found that tumor mass calculated using our MTC method was strongly correlated with lung weight in the murine orthotopic lung cancer model (r = 0.78), which demonstrates that our method can be used to accurately assess the growth of intra- and extra-parenchymal tumors in mice over time. We also found that tumor mass calculated with our MTC method was strongly correlated with the tumor burden calculated with all tested methods including the SCP method [17], whose process of using of bi-directional measurements to assess tumor response to therapy is similar to that used with RECIST and World Health Organization criteria. RECIST is the most common method used to estimate tumor burden in humans with cancer. We noticed that the MTC method outperformed the other four methods in the three mice with the highest tumor burdens as determined by lung weight. One of the possible reasons for this finding is that growing tumors sometimes meld together, making them difficult to distinguish, which leads to inaccurate estimations of tumor burden by methods that rely on the measurement of multiple individual tumors. The advantage of the MTC method over the four other tested methods is the accurate measurement of extra-parenchymal metastatic tumors in tumor burden calculation in a rapid manner.

The MTC method could be applied to assess tumor burden in GEMMs of lung cancer because GEMMs mimic human disease by the metastatic spread of *de novo* tumors in an immune-competent microenvironment. GEMM models are very important for studying lung cancer biology and for preclinical drug studies, as they have a tumor microenvironment that more closely reflects that in humans and thus could predict drug responses better than subcutaneous tumor models can. GEMMs are used to study the cellular processes that contribute to cancer initiation, progression, and metastasis. The GEMMs that recapitulate the natural history of human cancers and their clinical response to therapy constitute a major prerequisite for bench-to-bedside translation of investigational anticancer therapies and diagnostic imaging. Also, the evaluation of mouse models of lung cancer has improved our understanding of the genetic processes that lead to known genetic phenotypes of the disease, varying lung cancer histopathology, and certain tumor cell characteristics [34].

One limitation of our study is that the T&V method may not have been faithfully reproduced because the software used for that method is not commercially available. We used RayStation to calculate the tumor and vessel volume, and we used a threshold based on RayStation that is not the same as that suggested by Haines et al. [22]. A second limitation is that the measured mass using MTC might not include just tumor mass but also include blood mass due to thoracic hemorrhaging that occurs because of incorrect intubation and the extra-calcification of the rib cage. Lung obstruction with resulting lung collapse can also affect tumor measurement with all methods. Also, the presented method does not address a potential heterogeneity of treatment response in tumors, which would require identification and measurement of individual tumors at different times. We also did not histologically quantify tumors to determine the extent to which such measurements are correlated with tumor mass.

In conclusion, the findings of the present study demonstrate that our MTC method for the longitudinal assessment of lung cancer progression in murine models is unbiased, rapid, and accurate. Given that the software we used is commercially available, the method will be easy for others to reproduce. Combining this method with high-throughput micro-CT scanning in preclinical research could provide a rapid means of assessing tumor burden to help advance our understanding of lung cancer progression.

Acknowledgments

We thank Joe Munch in MD Anderson's Department of Scientific Publications for editing the manuscript.

References

[1] Siegel RL, Miller KD, and Jemal A (2018). Cancer statistics, 2018. *CA Cancer J Clin* **68**, 7–30.

[2] Hoffman RM (1999). Orthotopic metastatic mouse models for anticancer drug discovery and evaluation: a bridge to the clinic. *Investig New Drugs* **17**, 343–359.

[3] Killion JJ, Radinsky R, and Fidler IJ (1998). Orthotopic models are necessary to predict therapy of transplantable tumors in mice. *Cancer Metastasis Rev* **17**, 279–284.

[4] McLemore TL, Liu MC, Blacker PC, Gregg M, Alley MC, Abbott BJ, Shoemaker RH, Bohlman ME, Litterst CC, and Hubbard WC, et al (1987). Novel intrapulmonary model for orthotopic propagation of human lung cancers in athymic nude mice. *Cancer Res* **47**, 5132–5140.

[5] McLemore TL, Eggleston JC, Shoemaker RH, Abbott BJ, Bohlman ME, Liu MC, Fine DL, Mayo JG, and Boyd MR (1988). Comparison of intrapulmonary, percutaneous intrathoracic, and subcutaneous models for the propagation of human pulmonary and nonpulmonary cancer cell lines in athymic nude mice. *Cancer Res* **48**, 2880–2886.

[6] Goto H, Yano S, Zhang H, Matsumori Y, Ogawa H, Blakey DC, and Sone S (2002). Activity of a new vascular targeting agent, ZD6126, in pulmonary metastases by human lung adenocarcinoma in nude mice. *Cancer Res* **62**, 3711–3715.

[7] Onn A, Isobe T, Itasaka S, Wu W, O'Reilly MS, Ki Hong W, Fidler IJ, and Herbst RS (2003). Development of an orthotopic model to study the biology and therapy of primary human lung cancer in nude mice. *Clin Cancer Res* **9**, 5532–5539.

[8] Kwon MC and Berns A (2013). Mouse models for lung cancer. *Mol Oncol* **7**, 165–177.

[9] Guerra C, Mijimolle N, Dhawahir A, Dubus P, Barradas M, Serrano M, Campuzano V, and Barbacid M (2003). Tumor induction by an endogenous K-ras oncogene is highly dependent on cellular context. *Cancer Cell* **4**, 111–120.

[10] Jackson EL, Willis N, Mercer K, Bronson RT, Crowley D, Montoya R, Jacks T, and Tuveson DA (2001). Analysis of lung tumor initiation and progression using conditional expression of oncogenic K-ras. *Genes Dev* **15**, 3243–3248.

[11] Winslow MM, Dayton TL, Verhaak RG, Kim-Kiselak C, Snyder EL, Feldser DM, Hubbard DD, DuPage MJ, Whittaker CA, and Hoersch S, et al (2011). Suppression of lung adenocarcinoma progression by Nkx2–1. *Nature* **473**, 101–104.

[12] Gammon ST, Foje N, Brewer EM, Owers E, Downs CA, Budde MD, Leevy WM, and Helms MN (2014). Preclinical anatomical, molecular, and functional imaging of the lung with multiple modalities. *Am J Physiol Lung Cell Mol Physiol* **306**, L897–L914.

[13] Vande Velde G, De Langhe E, Poelmans J, Bruyndonckx P, d'Agostino E, Verbeken E, Bogaerts R, Lories R, and Himmelreich U (2015). Longitudinal in vivo microcomputed tomography of mouse lungs: No evidence for radiotoxicity. *Am J Physiol Lung Cell Mol Physiol* **309**, L271–L279.

[14] De Clerck NM, Meurrens K, Weiler H, Van Dyck D, Van Houtte G, Terpstra P, and Postnov AA (2004). High-resolution X-ray microtomography for the detection of lung tumors in living mice. *Neoplasia* **6**, 374–379.

[15] Cavanaugh D, Johnson E, Price RE, Kurie J, Travis EL, and Cody DD (2004). In vivo respiratory-gated micro-CT imaging in small-animal oncology models. *Mol Imaging* **3**, 55–62.

[16] Fushiki H, Kanoh-Azuma T, Katoh M, Kawabata K, Jiang J, Tsuchiya N, Satow A, Tamai Y, and Hayakawa Y (2009). Quantification of mouse pulmonary cancer models by microcomputed tomography imaging. *Cancer Sci* **100**, 1544–1549.

[17] Singh M, Lima A, Molina R, Hamilton P, Clermont AC, Devasthali V, Thompson JD, Cheng JH, Bou Reslan H, and Ho CC, et al (2010). Assessing therapeutic responses in Kras mutant cancers using genetically engineered mouse models. *Nat Biotechnol* **28**, 585–593.

[18] Namati E, Thiesse J, Sieren JC, Ross A, Hoffman EA, and McLennan G (2010). Longitudinal assessment of lung cancer progression in the mouse using in vivo micro-CT imaging. *Med Phys* **37**, 4793–4805.

[19] Rodt T, von Falck C, Dettmer S, Hueper K, Halter R, Hoy L, Luepke M, Borlak J, and Wacker F (2012). Lung tumour growth kinetics in SPC-c-Raf-1-BB transgenic mice assessed by longitudinal in-vivo micro-CT quantification. *J Exp Clin Cancer Res* **31**, 15–21.

[20] Rudyanto RD, Bastarrika G, de Biurrun G, Agorreta J, Montuenga LM, Ortiz-de-Solorzano C, and Munoz-Barrutia A (2013). Individual nodule tracking in micro-CT images of a longitudinal lung cancer mouse model. *Med Image Anal* **17**, 1095–1105.

[21] Li XF, Zanzonico P, Ling CC, and O'Donoghue J (2006). Visualization of experimental lung and bone metastases in live nude mice by X-ray micro-computed tomography. *Technol Cancer Res Treat* **5**, 147–155.

[22] Haines BB, Bettano KA, Chenard M, Sevilla RS, Ware C, Angagaw MH, Winkelmann CT, Tong C, Reilly JF, and Sur C, et al (2009). A quantitative volumetric micro-computed tomography method to analyze lung tumors in genetically engineered mouse models. *Neoplasia* **11**, 39–47.

[23] Gill BJ, Gibbons DL, Roudsari LC, Saik JE, Rizvi ZH, Roybal JD, Kurie JM, and West JL (2012). A synthetic matrix with independently tunable biochemistry and mechanical properties to study epithelial morphogenesis and EMT in a lung adenocarcinoma model. *Cancer Res* **72**, 6013–6023.

[24] Ungewiss C, Rizvi ZH, Roybal JD, Peng DH, Gold KA, Shin DH, Creighton CJ, and Gibbons DL (2016). The microRNA-200/Zeb1 axis regulates ECM-dependent beta1-integrin/FAK signaling, cancer cell invasion and metastasis through CRKL. *Sci Rep* **6**, 18652.

[25] Gibbons DL, Lin W, Creighton CJ, Rizvi ZH, Gregory PA, Goodall GJ, Thilaganathan N, Du L, Zhang Y, and Pertsemlidis A, et al (2009). Contextual extracellular cues promote tumor cell EMT and metastasis by regulating miR-200 family expression. *Genes Dev* **23**, 2140–2151.

[26] Rivera B, Bushman MJ, Beaver RG, Cody DD, and Price RE (2006). Breath-hold device for laboratory rodents undergoing imaging procedures. *J Am Assoc Lab Anim Sci* **45**, 54–59.

[27] Eisenhauer EA, Therasse P, Bogaerts J, Schwartz LH, Sargent D, Ford R, Dancey J, Arbuck S, Gwyther S, and Mooney M, et al (2009). New response evaluation criteria in solid tumours: revised RECIST guideline (version 1.1). *Eur J Cancer* **45**, 228–247.

[28] Schindelin J, Arganda-Carreras I, Frise E, Kaynig V, Longair M, Pietzsch T, Preibisch S, Rueden C, Saalfeld S, and Schmid B, et al (2012). Fiji: an open-source platform for biological-image analysis. *Nat Methods* **9**, 676–682.

[29] Dachman AH, MacEneaney PM, Adedipe A, Carlin M, and Schumm LP (2001). Tumor size on computed tomography scans: is one measurement enough? *Cancer* **91**, 555–560.

[30] Asteriti IA, De Mattia F, and Guarguaglini G (2015). Cross-talk between AURKA and Plk1 in Mitotic Entry and Spindle Assembly. *Front Oncol* **5**, 283–291.

[31] Sapi J, Kovacs L, Drexler DA, Kocsis P, Gajari D, and Sapi Z (2015). Tumor volume estimation and quasi-continuous administration for most effective bevacizumab therapy. *PLoS One* **10**e0142190.

[32] Ferrarotto R, Goonatilake R, Young Yoo S, Tong P, Giri U, Peng S, Minna J, Girard L, Wang Y, and Wang L, et al (2016). Epithelial-mesenchymal transition predicts polo-like kinase 1 inhibitor-mediated apoptosis in non-small cell lung cancer. *Clin Cancer Res* **22**, 1674–1686.

[33] Wang Y, Singh R, Wang L, Nilsson M, Goonatilake R, Tong P, Li L, Giri U, Villalobos P, and Mino B, et al (2016). Polo-like kinase 1 inhibition diminishes acquired resistance to epidermal growth factor receptor inhibition in non-small cell lung cancer with T790M mutations. *Oncotarget* **7**, 47998–48010.

[34] Safari R and Meuwissen R (2015). Practical use of advanced mouse models for lung cancer. *Methods Mol Biol* **1267**, 93–124.